



ELSEVIER

Available online at www.sciencedirect.com

SCIENCE @ DIRECT®

Powder Technology xx (2005) xxx – xxx

POWDER
TECHNOLOGY

www.elsevier.com/locate/powtec

Evaluation of lubrication force on colliding particles for DEM simulation of fluidized beds

Wenbin Zhang*, Reiji Noda, Masayuki Horio

Department of Chemical Engineering, Tokyo University of Agriculture and Technology, Koganei, Tokyo, 184-8588, Japan

Abstract

“Lubrication force” arises from hydrodynamic pressure in the interstitial fluid being squeezed out from the space between two solid surfaces. In the previous DEM simulations of gas–solid flows this force has not been explicitly taken into account since it may introduce the famous “Stokes Paradox”, which postulates that: Two solid surfaces can never make contact in a finite time in a viscous fluid due to the infinite “lubrication force” when the distance approaches zero at the last moment of contact. It is easy to imagine that lubrication effect is critical in liquid–solid systems, but it may not be negligible even in gas–solid systems of light and small particles. Although the lubrication theory has been well established in liquid–solid systems, its application in gas–solid systems should be used with caution because the assumptions adopted in the classical lubrication theory are only valid for high viscous systems. In the present study, these assumptions are examined and semi-theoretical expressions for lubrication force are proposed based on numerical analysis. The paradox of contactless collision due to infinite lubrication force is effectively avoided by considering surface roughness, non-continuum fluid effect and van der Waals force. The coefficient of restitution is defined as a criterion for evaluating the significance of lubrication effect in collisions of particles in fluidized beds. For demonstration the lubrication effect was evaluated for beds of FCC particles and GB (glass beads), with diameters ranging from 25 to 100 μm and initial approaching velocity from u_{mf} to u_t . The calculated restitution coefficient ranged from 0 to nearly 1 and clearly showed that lubrication force plays a significant role during a close encounter of two particles even in gas–solid systems.

© 2005 Published by Elsevier B.V.

Keywords: Lubrication force; DEM simulation; Collision; Stokes Paradox; Restitution coefficient

1. Introduction

The DEM (Discrete Element Method) treats the microscopic particle behavior by solving Newton’s equations of motion for each particle. It has become a popular tool for granular material simulation and has been applied to a variety of problems. The soft sphere model, which was first proposed by Cundall and Struck [1], was introduced to gas–solid systems by Tsuji [2] in 1993. Subsequently, Horio et al. [3–8] successfully applied the method to solve industrial issues relevant to fluidized beds for particle agglomeration, combustion with immersed tube and polymerization. However, there still remains a serious

empirism in how to include different interparticle forces in Newton’s equation of motion plausibly and also in how to adjust values such as the coefficient of restitution and the spring constant. To develop DEM further for more realistic simulation, a more accurate and practical collision model should be constructed in which the lubrication effect is included.

Lubrication force is a hydrodynamic viscous force arising from radial pressure in the interstitial fluid being squeezed from the space between two close solid surfaces. It originally received considerable attention in tribology (e.g. Briscoe and McClune [9]; Safa and Gohar [10]). Recently, researchers in the field of filtration and coagulation have also examined the elasto-hydrodynamic collisions between spherical particles. Davis [11] obtained both analytical and numerical solutions for collisions between two smooth spheres surrounded by thin isoviscous liquid layers with

* Corresponding author. Tel.: +81 42 388 7067; fax: +81 42 386 3303.

E-mail address: zhangwb@cc.tuat.ac.jp (W. Zhang).

54 consideration of dynamic deformation of particle surface.
 55 Subsequently, his research group developed the classical
 56 lubrication theory by taking into account the interparticle
 57 forces [12] and non-continuum fluid effect [13]. More
 58 recently, Thornton et al. [14] brought forward a simple
 59 analytical approximation based on a Hertzian-like profile for
 60 the elastic deformation of two spheres. Lian et al. [15]
 61 extended the lubrication theory to power-law fluid between
 62 rigid spheres and derived the analytical solutions for
 63 different flow index.

64 Although the lubrication theory was well established back
 65 in the 1900s, its application into DEM simulation of gas–
 66 solid flows has not been received sufficient attention. The
 67 well-known expression [11] for lubrication force
 68 $F_L = 6\pi\mu R^2 v/h$ indicates its relationship with fluid viscosity
 69 μ , particle radius R , relative approaching velocity v and
 70 surface distance h . As the viscosity of air is much lower
 71 than that of liquid, the lubrication force is generally
 72 considered to be negligible compared with gravity, hydro-
 73 dynamic drag force and interparticle forces. Moreover, the
 74 so-called “Stokes Paradox” that results in an infinite
 75 lubrication force when the surface distance approaches zero
 76 may also have been restricting its application to DEM
 77 simulations. Actually, however, even in gas–solid fluid-
 78 ization disregarding of lubrication effect is not acceptable
 79 for Geldart’s A and B powders with relatively small Stokes
 80 numbers. In the realistic collisions, we have several practical
 81 and essential reasons to avoid the paradox of contactless
 82 collision such as consideration of surface roughness, treat-
 83 ment of fluid as a non-continuum in the molecular scale and
 84 consideration of the effect of van der Waals force within
 85 very close surface distance. Among them, the effect of
 86 surface roughness is the most practical one because the
 87 existence of surface roughness effectively prevents particle
 88 surfaces from approaching much closer. And even if the
 89 surfaces are assumed to be ideally smooth, a minimum
 90 molecular distance Z_0 of about 4×10^{-10} m due to the
 91 molecular repulsion will remain when the surfaces make
 92 “physical” contact [16]. When two surfaces approach to
 93 such small distances, the interstitial fluid cannot be treated
 94 as a continuum any longer according to Hocking’s theory
 95 [17] and adhesive forces such as van der Waals force must
 96 be taken into account.

97 In the present work, the assumptions in the classical
 98 lubrication theory are re-examined since they were basically
 99 applicable for liquid–solid systems and semi-empirical
 100 expressions for lubrication force are proposed based on
 101 numerical calculations. According to the minimum
 102 approachable surface distance, three cases with and without
 103 considering non-continuum fluid effect and van der Waals
 104 force are investigated in order to construct a more accurate
 105 collision model. Calculated examples for restitution coef-
 106 ficient are presented for two typical bed materials often used
 107 in fluidized beds, FCC (Fluid Cracking Catalyst) particles
 108 and GB (glass beads) with diameters ranging from 25 to 100
 109 μm and initial approaching velocity from u_{mf} to u_t , to

110 evaluate the lubrication effect on the approaching process of
 111 two particles.

2. Theoretical development of lubrication theory 112

2.1. Examination of classical lubrication theory 113

114 As illustrated in Fig. 1, let us consider two identical
 115 elastic and spherical particles with radius R and mass m
 116 being immersed in a gaseous fluid and approaching each
 117 other. For the initial condition at $t=0$, we specify that the
 118 spheres start with a gap h_0 between their undeformed
 119 surfaces at $r=0$ and with a relative approaching velocity v_0 .
 120 The minimum surface distance that can be approached is
 121 denoted as h_{\min} . Only head-on collisions and no rotational
 122 movements are considered in this paper. And particles of the
 123 present interest are assumed to be rigid during approaching
 124 and separating stage according to Davis’ theory [11].

The kinematic equations of movement are listed below: 125

$$\frac{dh}{dt} = -v(t) = -(v_1 + v_2) \quad (1)$$

$$m \frac{dv}{dt} = -\sum F(t) = -F_L \quad (2)$$

126 where lubrication force F_L is considered to be the only
 127 dominant force in resultant force term when the surface
 128 distance is small compared with the particle radius.

129 The classical lubrication theory was originally estab-
 130 lished based on liquid–solid systems, in which the follow-
 131 ing assumptions were adopted: 132

- 133 (1) The initial gap size h_0 , from which lubrication effect is
 134 considered to be significant, is assumed to be much
 135 smaller than particle radius (usually $0.01 R$ [11]); 136
- 137 (2) The upper limit of integration of pressure for
 138 lubrication force is extended from particle radius to
 139 infinity; 140
- 141 (3) Paraboloid approximation of undeformed surface is
 142 applied in order to get the simplified gap profile.

$$H(r, t) = h(0, t) + r^2/R \quad (3)$$

- 143 (4) The fluid is treated as a continuum no matter how
 144 close the two surfaces approach. 145

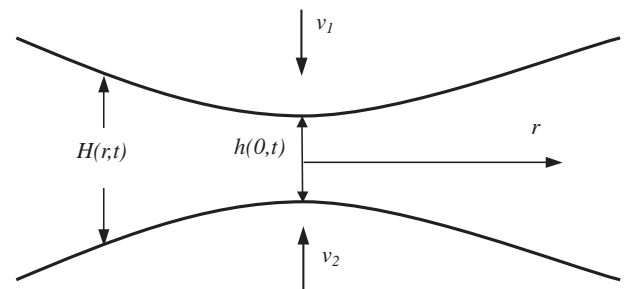


Fig. 1. Schematic of two approaching elastic and rigid spheres in a viscous fluid.

147 According to the classical lubrication theory (e.g. [11]),
 148 analytical expressions for interstitial pressure distribution
 149 and lubrication force can be derived as:

$$\frac{\partial p}{\partial r} = -\frac{6\mu rv}{H^3} \quad (4)$$

$$p(r,t) = \frac{3\mu Rv}{2(h+r^2/R)^2} \quad (5)$$

150

$$F_{L,\infty} = \int_0^\infty 2\pi rp(r,t)dr = \frac{3}{2}\pi\mu R^2v/h. \quad (6)$$

151

152 The radial pressure distribution expressed by Eq. (5)
 155 indicates that the pressure decays rapidly to zero within a
 156 small radial distance in the so-called “inner region”. The
 157 contribution of the pressure in the outer region to the
 158 integral of lubrication force can thus be reasonably
 159 neglected. Accordingly, the upper limit of integration can
 160 be effectively extended from R to infinity just to obtain the
 161 simplified analytical form of lubrication force. Also, within
 162 this small inner region, paraboloid approximation is
 163 sufficiently accurate.

164 However, these assumptions may not remain reasonable
 165 with regard to particle collisions in gas–solid systems.
 166 Among them, the initial gap size h_0 should be firstly
 167 checked to define the lubrication effect area. Order-of-
 168 magnitude estimates of different forces in case of FCC
 169 particles with radius of $25\ \mu\text{m}$ and approaching velocity of
 170 terminal velocity u_t are indicated in Fig. 2. The drag force
 171 F_d was calculated under laminar conditions with a Reynolds
 172 number of about 0.293. An effective drag coefficient
 173 $C_D = C_{D0}\varepsilon^{-4.65}$ was adopted with a bed voidage ε of 0.9. It
 174 can be seen that from $h_0=R$ the lubrication force should be
 175 taken into account compared with other forces such as
 176 gravity G and drag force F_d . The results agree well with
 177 Brenner’s exact solutions [18] and hybrid approximation
 178 suggested by Leighton [19]. Thus, the particle radius can be
 179 regarded as a characteristic distance to judge whether the

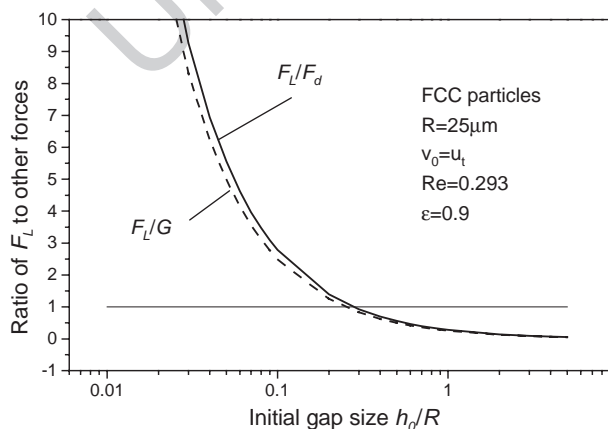


Fig. 2. Order-of-magnitude estimates of different forces.

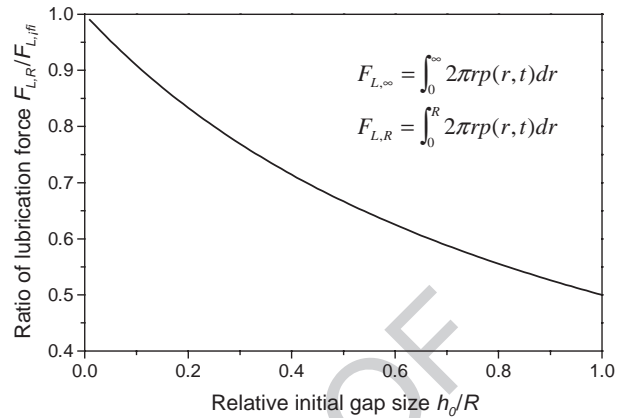


Fig. 3. Comparison of lubrication force applying different upper limit for integration (FCC particles, in air, $R=25\ \mu\text{m}$, $v_0=u_t=0.098\ \text{m/s}$).

two particles have entered the so-called “lubrication effect area” or “near contact area”, in which lubrication force should be included in the Newton’s equation of motion. Out of this near contact area where particles are separated from each other widely, particle movements are dominated by hydrodynamic drag force and gravity, with lubrication force being neglected.

Fig. 3 shows the ratio of lubrication force integrated with different upper limit changing with the relative initial gap size. The actual lubrication force should be integrated over the particle surface:

$$F_{L,R} = \int_0^R 2\pi rp(r,t)dr. \quad (7)$$

From Fig. 3, we can see that when h_0 is much smaller than the particle radius, the difference is not so significant. However, when h_0 increases to as large as the particle radius, the actual lubrication force from Eq. (7) is only half of that integrated from zero to infinity by Eq. (6). Therefore, the adoption of the upper limit as infinity is unreasonable when the lubrication effect area is as large as the particle radius R .

For estimation of the error introduced by paraboloid approximation, numerical calculations for accurate pressure distribution and lubrication force were conducted under different initial gap size. Without the paraboloid approximation, the distance $H(r,t)$ between particle surfaces has the following accurate expression:

$$H(r,t) = h(0,t) + 2R - 2\sqrt{R^2 - r^2}. \quad (8)$$

By combining Eq. (8) with Eq. (4), one can obtain the pressure distribution numerically.

Fig. 4 shows that the numerical pressure distribution decays to zero much more slowly than the analytical solution. The contribution of pressure in the outer region to the lubrication force may play an important role

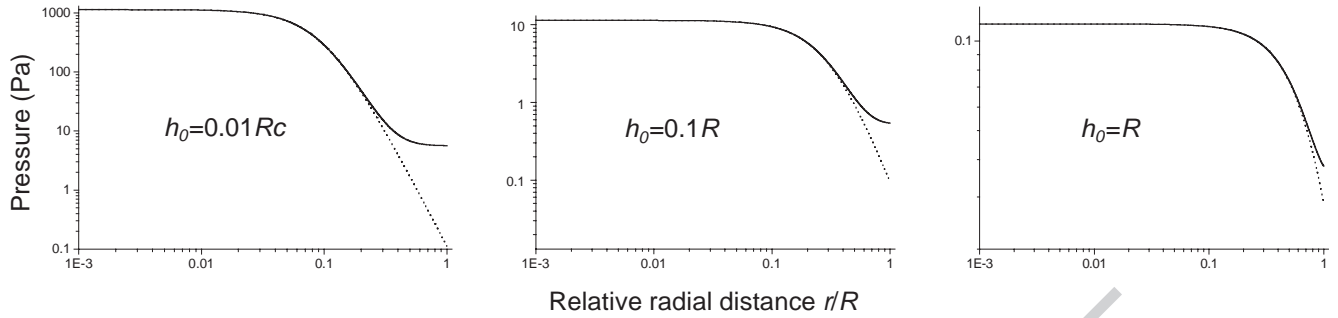


Fig. 4. Comparison of pressure distribution between numerical and analytical solutions (solid line: numerical solutions calculated from Eqs. (4) and (8); dotted line: analytical solutions calculated from Eq. (5)).

215 especially when h_0 is much smaller than particle radius. The
 216 relative magnitude of analytical and numerical solution for
 217 lubrication force along the radial direction is shown in Fig.
 218 5. The analytical expression for lubrication force with
 219 various integration upper limits is based on paraboloid
 220 approximation.

$$F_{L,r,ana} = \int_0^r 2\pi r p(r,t) dr = \frac{3}{2} \pi \mu R^2 v \left(\frac{1}{h} - \frac{1}{h + r^2/R} \right). \quad (9)$$

223 Variation of $F_{L,r,ana}$ with radial distance indicates the
 224 contribution of pressure within different radial distance to
 225 the lubrication force. We define the radial distance r^* as
 226 the radius of inner region and suppose that, within this
 227 inner region, the analytical solution has an accuracy of
 228 90% of the accurate numerical solution. We found that the
 229 inner region expanded with the increase of gap size, thus
 230 making the analytical solution convincing in a wider
 231 region. When $h=R$, the analytical solution agrees well
 232 with the numerical one in the whole integration range from
 233 zero to R .

234 Finally, in gas–solid systems, the mean free path l_0 of
 235 gaseous molecules is in the order of 10^{-7} m, which is much
 236 larger than that of liquid molecules. Therefore, the
 237 assumption that the fluid remains a continuum may be
 238 broken when the surface distance is approached to such a
 239 magnitude that is comparable to the mean free path.

240 With the examination of the assumptions adopted in
 241 liquid–solid systems, we found that all of them were not

valid when gas–solid systems are concerned. The exact
 surface distance, pressure profile and lubrication force
 should be solved numerically by combining Eqs. (4), (7)
 and (8).

2.2. Lubrication force and avoidance of “Stokes Paradox”

In the collision process between practical particles with
 roughness, the minimum approachable surface distance h_{min}
 is assumed to be determined by the height of surface
 roughness h_r . Accordingly, the maximum lubrication force
 corresponding to the moment at which physical contact
 occurs depends on the surface morphology of particles.
 When the surface roughness is of the same order of the mean
 free path of gaseous molecules, the interstitial fluid should be
 treated as a non-continuum. What’s more, when its
 magnitude is comparable to the dominant range of adhesive
 forces, the effect of such forces on collision must be taken
 into account. According to the relative magnitude of
 minimum approachable surface distance h_{min} , three cases
 are discussed below.

Case 1. $h_{min} > l_0$

In this case, particles have large surface roughness that is
 much larger than the mean free path l_0 and the interstitial
 fluid can be reasonably regarded as a continuum.

Based on the numerical calculation results, the ratio of
 numerical solution to analytical one for lubrication force is
 found to be a function of the relative approaching distance

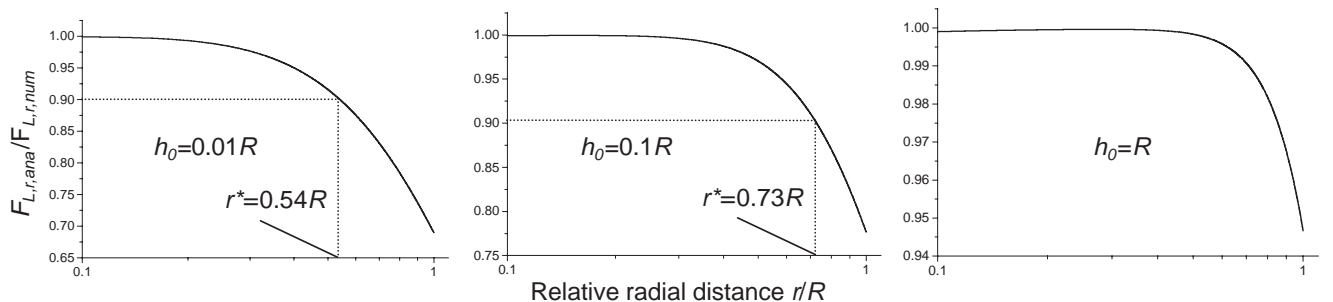


Fig. 5. Comparison of numerically and analytically calculated lubrication force with various integration upper limit. $F_{L,r,ana} = \int_0^r 2\pi p_1(r,t) dr$, where $p_1(r,t)$ has the analytical form of Eq.(5). $F_{L,r,num} = \int_0^r 2\pi p_2(r,t) dr$, where $p_2(r,t)$ is the numerically solved from Eqs.(4) and (8).

269 h/R . The relationship curve can be fitted by a two-order
 270 polynomial correlation with an error smaller than 1.5% in
 271 the range of $0.01 < h/R < 1$ (see Fig. 6).

$$K_1(h) = \frac{F_{L,num}}{F_{L,ana}} = 1.041 - 0.2811g \frac{h}{R} - 0.0351g^2 \frac{h}{R} \quad (10)$$

273 where $F_{L,ana}$ is the analytical expression for lubrication
 274 force integrated over the particle surface with paraboloid
 275 approximation.

$$F_{L,ana}(h) = \int_0^R 2\pi r p dr = \frac{3}{2} \pi \mu R^2 v \left(\frac{1}{h} - \frac{1}{h+R} \right). \quad (11)$$

276 Since the surface distance is unable to approach zero due
 277 to the prevention of surface roughness, the continuous
 278 increase of lubrication force in the approaching process is
 279 stopped when the tip of roughness makes contact. Hence,
 282 the infinite lubrication force cannot be reached and the
 283 “Stokes Paradox” is accordingly avoided.

284 **Case 2.** $Z_0 < h_{min} < l_0$

285 Particles in this case have smaller surface roughness
 286 compared with the mean free path. So the non-continuum
 288 fluid effect should be considered in the last stage of
 289 approaching.

290 Maxwell slip theory, which was initially introduced by
 291 Hocking [17] in 1973, is adopted in the present paper to
 292 treat the interstitial fluid as a non-continuum. Different
 293 from Eq. (4) for continuum fluid case, the pressure
 294 profile in the non-continuum fluid can be expressed by
 295 [17]:

$$\frac{\partial p}{\partial r} = - \frac{6\mu r v}{H^2(H + 6l_0)} \quad (12)$$

296 where l_0 is the mean free path of gaseous molecules.

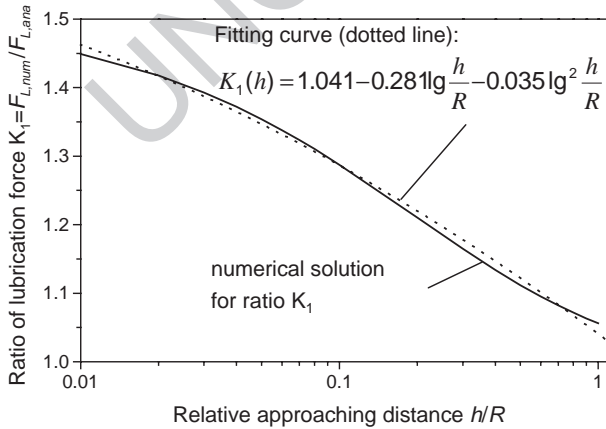


Fig. 6. Fitting curve of the ratio of numerical lubrication force to an analytical one (FCC particles, in air, $R=25 \mu\text{m}$, $v_0=u_t$, $h_0=R$, $F_{L,ana}$ is calculated from Eq. (11) with paraboloid approximation). Numerical solution for ratio K1 Fitting curve (dotted line).

Similarly with Case 1, another semi-empirical correlation
 is proposed here with a relative error smaller than 1% in the
 range of $h/R < 0.01$.

$$K_2(h) = \frac{F_{L,num,slip}}{F_{L,ana,slip}} = 1.309 - 0.0821g \frac{h}{R} - 0.0091g^2 \frac{h}{R} \quad (13)$$

$$F_{L,ana,slip} = \frac{\pi \mu R^2 v}{12l_0^2} \left[(h + 6l_0) \ln \left(\frac{h + 6l_0}{h} \right) - (h + R + 6l_0) \times \ln \left(\frac{h + R + 6l_0}{h + R} \right) \right]. \quad (14)$$

From Eq. (14) we can find that when $l_0 \ll h$, the
 expression of $F_{L,ana,slip}$ converges to $F_{L,ana}$ in Eq. (11),
 and when $l_0 \gg h$, the expression of $F_{L,ana,slip}$ converges to:

$$F_{L,ana,slip} = \frac{\pi \mu R^2 v}{2l_0} \ln \left(\frac{6l_0}{h} \right), \quad l_0 \gg h. \quad (15)$$

The above expression shows that the increase of the
 lubrication force is slowed down because its magnitude is
 only proportional to the logarithm of the inverse of the gap
 size. Therefore, treatment of the fluid as a non-continuum
 also helps us avoid the paradox of the infinite lubrication
 force.

Case 3. h_{min} is comparable to Z_0

When the surface roughness is so small that the
 minimum approachable distance is of the same order of
 the repulsive molecular distance $Z_0 = 4 * 10^{-10} \text{ m}$, which is
 the dominant range of adhesive forces, these forces such as
 van der Waals force F_{vw} should be taken into account. In
 this case, the van der Waals force ought to be included in the
 resultant force term in the kinematic Eq. (2).

$$m \frac{dv}{dt} = - \sum F(t) = - (F_L - F_{vw}) \quad (16)$$

where lubrication force F_L can be calculated by applying
 Eq. (13) with the approximation of K_2 to be 1.5, and van der
 Waals force F_{vw} is expressed by

$$F_{vw} = - \frac{AR}{12h^2} \quad (17)$$

where A is the Hamaker constant of the particle material.

As van der Waals force is inversely proportional to the
 square of the distance, its magnitude increases dramatically
 when the distance approaches Z_0 . The variation of
 lubrication force, van der Waals force and the resultant net
 force along with surface distance are shown in Fig. 7. Under
 the condition that the net force $F_{net} = F_L - F_{vw} = 0$, we
 define a critical “collapse distance” $h_{collapse}$, above which
 the particles resist approaching to each other due to the
 lubrication force but below which, on the contrary, the

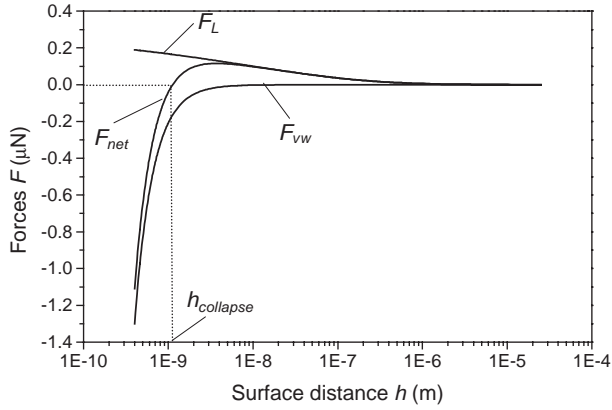


Fig. 7. Variation of lubrication force, van der Waals force and resultant net force with approaching surface distance (GB particles, $d_p=50 \mu\text{m}$, $v_0=u_t/5$, $h_0=R$).

339 particles collapse and make contact in the aid of van der
340 Waals force. Therefore, the consideration of van der Waals
341 force in the very last approaching stage essentially saves us
342 from the paradox of contactless collision.

343 The collapse distance can be solved from the following
344 equation:

$$\frac{3}{4} \frac{\pi \mu R^2 v}{l_0} \ln \frac{6l_0}{h_{\text{collapse}}} = \frac{AR}{12h_{\text{collapse}}^2} \quad (18)$$

345 In the case of GB with diameter of $50 \mu\text{m}$ and
346 approaching velocity of $u_t/5$, this collapse distance can be
347 estimated to be $h_{\text{collapse}}=10^{-9} \text{m}$.

348 By deriving the relationship of relative velocity with
349 surface distance and substituting it into Eq. (18), we can get
350 the dimensionless correlation:

$$\hat{E} St^2 = \frac{1}{4} \frac{l_0}{Z_0} \hat{h}_{\text{collapse}}^2 \ln \frac{6}{\hat{h}_{\text{collapse}}} \left(St + \frac{1}{4} \hat{h}_0 \ln \frac{\hat{h}_0}{16.3} \right) \quad (19)$$

351 where the dimensionless parameters are defined as:

$$\hat{h} = \frac{h}{l_0}, \quad St = \frac{mv_0}{6\pi\mu R^2}, \quad \hat{E} = \frac{E}{\frac{1}{2}mv_0^2} = \frac{AR}{6Z_0mv_0^2} \quad (20)$$

352 where E is the depth of the attractive potential well due to
353 van der Waals force:

$$E = - \int_{Z_0}^{\infty} \frac{AR}{12h^2} dh = \frac{AR}{12Z_0} \quad (21)$$

354 \hat{h} is the relative distance compared with the mean free
355 path, Stokes number, St , provides a measure of the inertia of
356 an isolated particle relative to the viscous force and \hat{E} is the
357 dimensionless adhesion energy compared with initial kinetic
358 energy.

359 Fig. 8 shows contours of the collapse distance with
360 dimensionless parameters. The Y-coordinate $\hat{E}St^2 =$

361 $\frac{A}{216\pi^2 Z_0 \mu^2 R^3}$ represents only the physical properties of
362 fluid and particles, being independent of approaching
363 velocity. With respect to a certain condition of particle
364 and fluid, the collapse distance decreases with increase
365 of Stokes number, indicating that the lubrication force
366 dominates the particles' movement when the Stokes
367 number of particles is large. Under the constant Stokes
368 number, the collapse distance increases with increase of
369 dimensionless adhesive energy \hat{E} . This means that with
370 increasing Hamaker constant, the dominant range of van
371 der Waals force which is smaller than h_{collapse} expands
372 wider.

2.3. Effective restitution coefficient

373 The lubrication effect is actually a kind of damping
374 effect, causing kinetic energy dissipation during both
375 approaching and separating stage. Restitution coefficient,
376 which represents the energy loss during collision process, is
377 usually defined as the ratio of the normal relative velocity at
378 the instant of rebound to that at the instant of contact.
379 However, if we consider that the collision process begins
380 when the particles enter the lubrication effect area and ends
381 when the surface distance recovers to the initial gap size, the
382 definition of restitution coefficient can be extended as the
383 ratio of normal velocity at the instant of escaping from this
384 area (v_e) to that at the instant of entering this area (v_0). Thus
385 restitution coefficient can be regarded as a criterion for
386 evaluating the lubrication effect during approaching and
387 separating process.

388 Combining Eqs. (1), (2), (10)–(14) to eliminate the time
389 term and integrating in the approaching and separating
390 stage, we can obtain the expression for the restitution
391 coefficient e .

$$e = e_c - \frac{1 + e_c}{2St} St_e^* \quad (22)$$

392 where e_c is the restitution coefficient due to particle
393 deformation in the collision process. If we assume that the

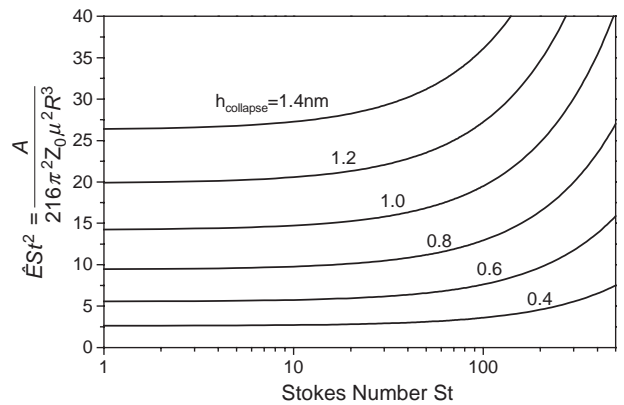


Fig. 8. Contour of collapse distance with dimensionless parameters (GB, in air, $R=25 \mu\text{m}$, range of $St: 1 \sim 500$).

402 collision process is an elastic one with e_c being equal to
403 unity, Eq. (22) can be simplified into:

$$e = 1 - \frac{St_c^*}{St} = 1 - \frac{2St_c^*}{St} \quad (23)$$

404 where the two critical Stokes number are defined as:

$$St_c^* = \frac{mv_c^*}{6\pi\mu R^2}, \quad St_c^* = \frac{mv_e^*}{6\pi\mu R^2} \quad (24)$$

406 where v_c^* is called “critical contact velocity”. Particles with
408 initial approaching velocity v_0 smaller than v_c^* cannot make
409 contact due to the repulsive lubrication force; v_e^* is called
410 “critical escape velocity”. Particles with $v_0 > v_e^*$ but $v_0 < v_c^*$,
411 however have sufficient kinetic energy to make contact, yet
412 cannot escape from the lubrication effect area due to the
413 attractive lubrication force during the separating stage and
414 will be brought to rest.

415 By derivation, St_c^* has the following expression:

$$St_c^* = f(h_0) - f(h_{\min}) = 2St_c^* \quad (25)$$

416 where $f(h)$ is called “characteristic function”, h_0 is
418 considered to be equal to particle radius and h_{\min} is
419 practically determined by surface roughness.

420 For Case 1 with continuum fluid:

$$f_1(h) = 0.962 \ln\left(\frac{h}{h+R}\right) - 0.079 \ln^2\left(\frac{h}{h+R}\right) - 0.004 \ln^3\left(\frac{h}{h+R}\right). \quad (26)$$

423 For Case 2 with non-continuum fluid:

$$f_2(h) = \frac{1}{36} \left(6 + \frac{h}{l_0}\right)^2 \ln\left(1 + \frac{6l_0}{h}\right) - \frac{1}{36} \left(6 + \frac{h+R}{l_0}\right)^2 \ln\left(1 + \frac{6l_0}{h+R}\right) - \ln\left(1 + \frac{R}{h}\right) - \frac{R}{6l_0}. \quad (27)$$

426 For Case 3 with non-continuum fluid and van der Waals
427 force:

$$St_c^* = f_3(h_0) - f_3(h_{\text{collapse}}), \quad f_3(h) = f_2(h). \quad (28)$$

429 In Case 3, the characteristic function $f_3(h)$ is the same as
431 that for Case 2 (Eq. (27)). However, the minimum
432 approachable distance h_{\min} in Eq. (25) should be replaced
433 by the collapse distance h_{collapse} because particles with
434 enough inertia to approach h_{collapse} can further make contact
435 in the aid of van der Waals force even if the velocity at this
436 moment has decreased to zero. Nevertheless, the effect of
437 van der Waals force on the restitution coefficient is not so
438 significant since most of the energy loss is dissipated by
439 lubrication force before they nearly make contact. This can

also be demonstrated by the similar value of $f_2(h_{\min})$ and
 $f_3(h_{\text{collapse}})$ in Eqs. (25) and (28).

3. Calculated examples and discussion

In the present paper, two typical powders for fluidized bed
processes, i.e., FCC particles and GB (Glass Bead), are
adopted to evaluate the lubrication effect on collision
process. The particle size ranges from 25 to 100 μm
corresponding to Geldart’s A and B classification and the
initial approaching velocity varies from u_{mf} to u_t . The
physical properties of particles and fluid are listed in Table 1.

3.1. Case 1: FCC particles with large surface roughness

From observation of the surface morphology of FCC
particles by laser microscopy, the surface roughness of each
tested particle is approximately one tenth of the particle
radius. Within the range of particle size investigated in this
paper, h_{\min} is much larger than the mean free path of air
molecules. Therefore, the interstitial fluid can be reasonably
treated as a continuum in the case of FCC particles.

Fig. 9 shows the variation of lubrication force and
relative velocity during the approaching and separating
stage with the surface distance. At the moment when the
surface distance equals to the surface roughness, physical
contact between the surfaces occurs. Subsequently, the
separating stage begins until the surface distance returns to
the initial value h_0 . Due to the energy dissipation by the
lubrication force both in approaching and separating stage,
the relative velocity keeps decreasing in the whole process.
Lubrication force increases more rapidly when the surfaces
approach closer. At the moment of contact in this example,
its magnitude increases to a maximum value which is about
20 times of its initial value at $h = h_0$.

Fig. 10 shows how restitution coefficient varies with
initial approaching velocity ranging from u_{mf} to u_t . Results
applying classical lubrication theory are also displayed using

Table 1

Physical properties of particles and fluid

	FCC	GB	
<i>Particles</i>			t1.1
Particle diameter d (μm)	25~100	25~100	t1.2
Particle density ρ_p (kg/m^3)	1400	2650	t1.3
Young’s Modulus E (N/m^2)	1.0×10^{11}	8.0×10^{10}	t1.4
Poisson’s ratio ν	0.28	0.3	t1.5
Roughness h_r (m)*	1/10 of the particle radius	1/1000 of the particle radius	t1.6
Hamaker constant A (J)	–	1.0×10^{-19}	t1.7
<i>Fluid: Air at $p=1$ atm, $T=300$ K</i>			t1.8
Viscosity μ (Pa s)	1.94×10^{-5}		t1.9
Density ρ_f (kg/m^3)	1.16		t1.10
Mean free path l_0 (m)	7.15×10^{-8}		t1.11

* Surface roughness of particles is estimated based on the optical
observation of surface morphology using laser microscopy and SEM.

t1.16

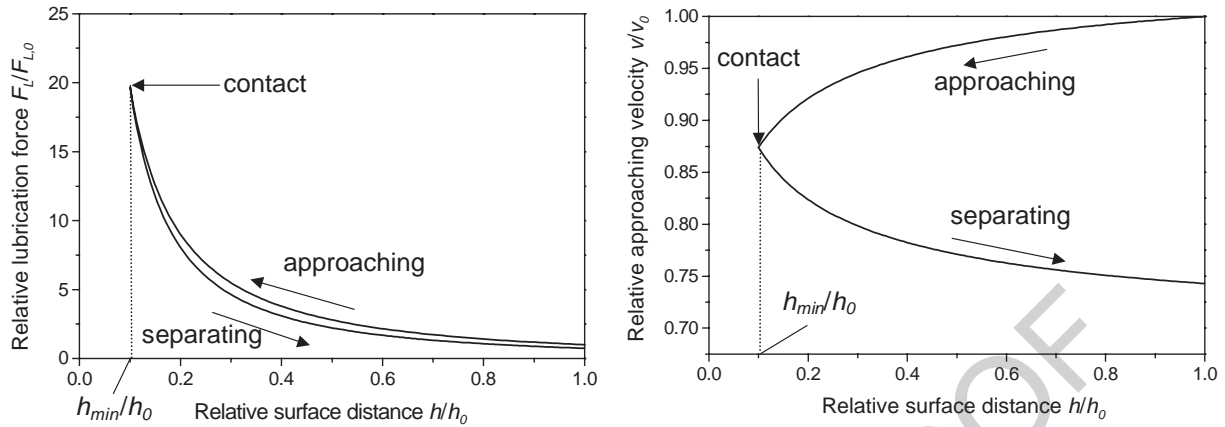


Fig. 9. Variation of lubrication force and approaching velocity with relative surface distance (FCC particles, $d_p=50 \mu\text{m}$, $v_0=u_t/5$, $h_0=R$, $h_{\min}=h_r=0.1 R$).

474 dotted lines for comparison. With the increase of initial
 475 velocity, restitution coefficient approaches to unity, indicat-
 476 ing that lubrication effect is not so significant at high
 477 velocities. Nevertheless, when the initial velocity is smaller
 478 than the critical escape velocity v_c^* , e decreases to zero.
 479 Particles with initial velocity of u_{mf}^* and $u_t/50$ which are
 480 smaller than v_c^* do not have enough inertia to make contact
 481 and will come to rest in the approaching stage. Yet particles
 482 with an initial velocity of $u_t/20$ can make contact but do not
 483 have enough inertia to escape from the “lubrication effect
 484 area” and will come to rest in the separating stage. Therefore,
 485 collisions with an initial approaching velocity less than v_c^*
 486 will result in agglomeration. The results calculated by
 487 classical lubrication theory show a similar tendency and
 488 smaller values of a restitution coefficient due to the
 489 assumption of the upper limit of infinity in the integration
 490 of the lubrication force.

491 Results of restitution coefficient with different particle
 492 size and different initial approaching velocity are shown in
 493 Fig. 11. It can be found that under the same initial velocity,
 494 the effect of the lubrication force on larger particles is less
 495 significant than on smaller particles. The independent
 496 effects of particle size and initial approaching velocity on

the collision process can be included in the consideration of
 Stokes numbers. As can be seen from Fig. 12, the effect of
 lubrication force on particles with larger St is less
 significant. The lubrication effect can be completely
 neglected when the Stokes number is larger than 1000.
 Fig. 12 also shows the influence of different surface
 roughness on the restitution coefficient. For the same Stokes
 number, the lubrication effect on the collision is more
 significant in case of smoother particles.

3.2. Case 2: GB with small surface roughness

Glass beads with surface roughness that is approximately
 equal to 1/1000th of the particle radius are much smoother
 than FCC particles. The particle surfaces can approach to a
 much closer distance so that the lubrication effect is more
 significant and the fluid should be treated as a non-
 continuum in the last approaching stage.

Fig. 13 shows the comparison of lubrication force along
 with surface distance with and without considering the non-
 continuum fluid effect. It can be seen that the magnitude of
 lubrication force decreases greatly when the surface distance
 is of the same order of a mean free path of air by taking into

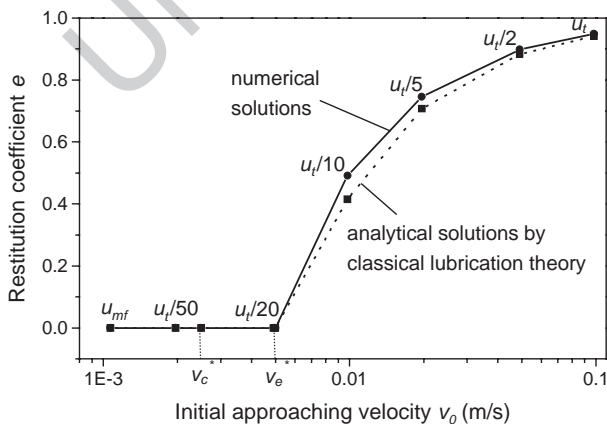


Fig. 10. Variation of restitution coefficient with initial approaching velocity (FCC particles, $d_p=50 \mu\text{m}$, $h_0=R$, $h_{\min}=h_r=0.1 R$).

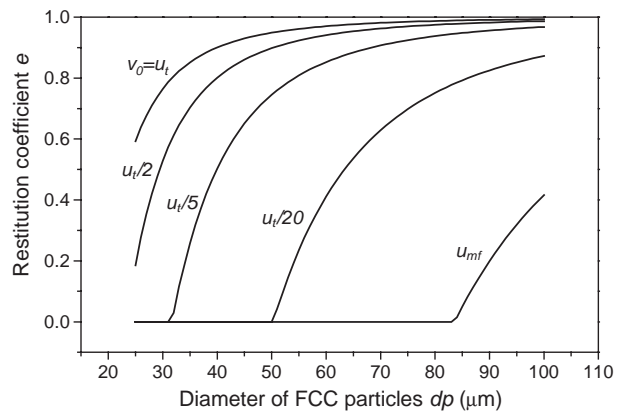


Fig. 11. Restitution coefficient with different size of FCC particles and different initial approaching velocity (FCC particles, $h_0=R$, $h_{\min}=h_r=0.1 R$, velocity range: $u_{mf} \sim u_t$; diameter range: 25~100 μm).

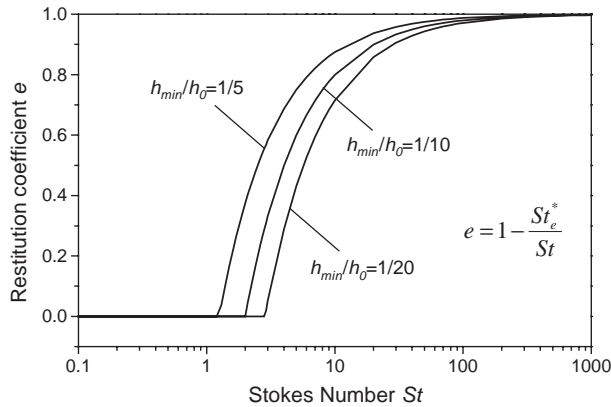


Fig. 12. Variation of restitution coefficient with Stokes numbers and different surface roughness (FCC particles, $h_0=R$, $h_{min}=h_r$).

518 account the non-continuum fluid effect. Therefore, treatment
 519 of the fluid as a non-continuum in the last approaching stage
 520 significantly slows down the increase of lubrication force to
 521 infinity.

522 A comparison of the restitution coefficient of different
 523 sized GB under different initial approaching velocities is
 524 shown in Fig. 14. Results indicate that lubrication effect on
 525 GB collisions cannot either be neglected especially for
 526 smaller particles and lower initial approaching velocity. The
 527 differences of restitution coefficient with and without non-
 528 continuum effect also indicate that consideration of non-
 529 continuum effect weakens the lubrication effect and thus
 530 lead to an increase in the restitution coefficient.

531 3.3. Case 3: smooth GB without surface roughness

532 In most DEM simulations, GB is assumed to be ideally
 533 smooth without surface roughness. However, even in this
 534 case, the paradox of contactless collision can be essentially
 535 avoided by the attractive interaction of adhesive forces in the
 536 range of distance smaller than $h_{collapse}$. This collapse distance
 537 $h_{collapse}$ can thus be regarded as the minimum approachable
 538 surface distance h_{min} .

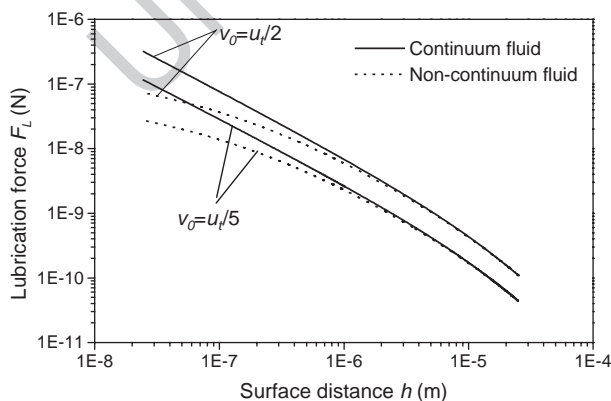


Fig. 13. Variation of lubrication force with surface distance applying continuum fluid model and non-continuum fluid model (GB particles, $d_p=50 \mu m$, $h_0=R$, $h_{min}=h_r=0.001 R$).

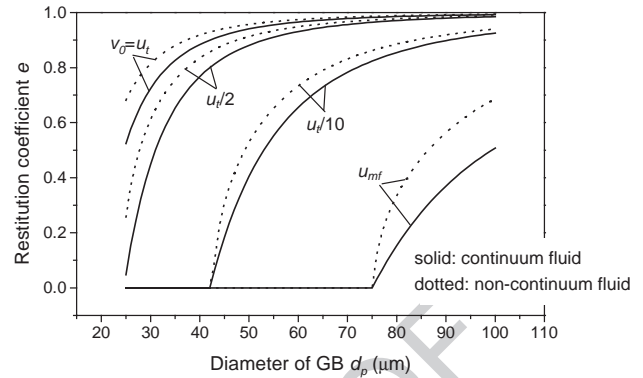


Fig. 14. Comparison of restitution coefficient calculated by continuum and non-continuum fluid model (GB particles, $h_0=R$, $h_{min}=h_r=0.001 R$ velocity range: $u_{mf} \sim u_i$; diameter range: $25 \sim 100 \mu m$).

539 Fig. 15 shows the calculated results of the restitution
 540 coefficient with and without considering the effects of non-
 541 continuum fluid and van der Waals force. Comparing with
 542 Fig. 14, we can find that the differences between two sets of
 543 results are much larger because, with the assumption of
 544 smooth GB surface, particles can approach more closely so
 545 that the effect of non-continuum fluid may be more
 546 significant.

547 4. Conclusions

548 Although the classical lubrication theory has been well
 549 established in liquid–solid systems, its application into
 550 gas–solid systems has not received enough attention. The
 551 assumptions adopted in the previous lubrication theory do
 552 not remain reasonable as to gas–solid systems based on the
 553 numerical analysis. The lubrication effect area in gas–solid
 554 systems can be as large as the particle radius. The numerical
 555 calculation results show that the pressure distribution in the
 556 outer region cannot be neglected and their contribution to
 557 lubrication force is related to the relative surface distance.
 558 Semi-empirical expressions for lubrication force with and

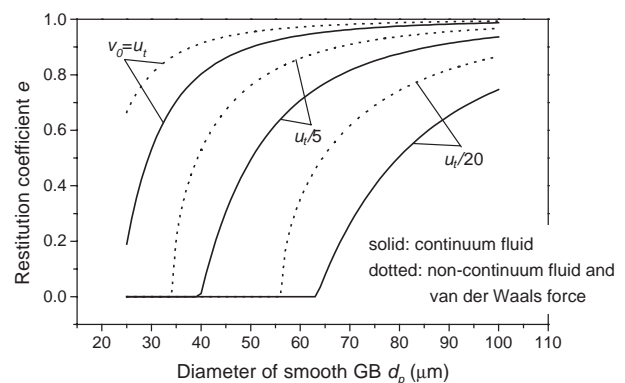


Fig. 15. Restitution coefficient with and without non-continuum fluid effect and van der Waals force (GB particles, $h_0=R$, $h_{min}=h_{collapse}$, velocity range: $u_{mf} \sim u_i$; diameter range: $25 \sim 100 \mu m$).

559 without considering non-continuum fluid effect are pro-
560 posed according to the numerical analysis.

561 Surface roughness of practical particles helps us avoid
562 the classical “Stokes Paradox” since it prevents particles
563 from approaching to a closer distance. Moreover, in the last
564 approaching stage where the surface distance is of the order
565 of the mean free path of fluid, the interstitial fluid should be
566 treated as a non-continuum, thus slowing down the increase
567 of lubrication force. Finally, within a critical collapse
568 distance where van der Waals force dominates over
569 lubrication force, the paradox of contactless collision is
570 essentially avoided since the particles can be driven together
571 to make contact in the aid of van der Waals force.

572 Restitution coefficient is adopted as a criterion for
573 evaluating the lubrication effect on collision process. It is a
574 strong function of Stokes number of isolated particle and
575 critical Stokes number that can be determined by corre-
576 sponding characteristic functions. The lubrication effect is
577 more pronounced for particles with smaller Stokes numbers.
578 Calculation results clearly show that the lubrication effect
579 cannot be neglected during the collision process in gas–solid
580 systems with FCC and GB of particle sizes ranging from 25
581 to 100 μm and initial approaching velocity from u_{mf} to u_t .
582 Further research should be aiming at incorporating
583 lubrication force and an effective restitution coefficient
584 defined in this paper into DEM simulations with a more
585 accurate collision model.

586 Nomenclature

587 A	Hamaker constant, J
588 d_p	Particle diameter, μm
589 E	Attractive potential, J
590 e	Restitution coefficient in Eq. (22)
591 e_c	Restitution coefficient by deformation
592 F_d	Drag force, N
593 F_L	Lubrication force, N
594 F_{vw}	Van der Waals force, N
595 F_{net}	Resultant net force, N
596 G	Gravity, N
597 H	Surface distance, m
598 h	Surface distance at $r=0$, m
599 h_0	Initial surface distance at $r=0$, m
600 h_{min}	Minimum surface distance, m
601 h_r	Surface roughness, m
602 h_{collapse}	Critical collapse distance, m
603 K_1	Correction factor in Eq. (10)
604 K_2	Correction factor in Eq. (13)
605 l_0	Mean free path of molecules, m
606 m	Particle mass, kg
607 P	Hydrodynamic pressure, Pa
608 R	Particle radius, m
609 r	Radial distance in Fig. 1, m
610 r^*	Radius of inner region, m
611 St	Stokes number
612 St_c^*	Critical contact Stokes number
673	

St_c^*	Critical escape Stokes number	613
u_{mf}	Minimum fluidized velocity, m/s	614
u_t	Terminal velocity, m/s	615
v	Relative approaching velocity, m/s	616
v_0	Initial approaching velocity, m/s	617
v_c^*	Critical contact velocity, m/s	618
v_e^*	Critical escape velocity, m/s	619
Z_0	Repulsive molecular distance, m	620

Greek letters

ε	Bed voidage	621
μ	Viscosity of fluid, Pa s	622
ρ_p	Particle density, kg/m^3	623
ρ_f	Fluid density, kg/m^3	624
		625
		626

References

- | | | |
|------|--|-----|
| | | 627 |
| | | 628 |
| [1] | P.D. Cundall, O.D.L. Struck, A discrete numerical model for granular assemblies, <i>Geotechnique</i> 29 (1979) 47. | 629 |
| [2] | Y. Tsuji, T. Kawaguchi, T. Tanaka, Discrete particle simulation of two-dimensional fluidized bed, <i>Powder Technol.</i> 77 (1993) 79. | 630 |
| [3] | T. Mikami, H. Kamiya, M. Horio, Numerical simulation of cohesive powder behavior in a fluidized bed, <i>Chem. Eng. Sci.</i> 53 (1998) 1927. | 631 |
| [4] | Y. Kaneko, T. Shiojima, M. Horio, DEM simulation of fluidized beds for gas-phase olefin polymerization, <i>Chem. Eng. Sci.</i> 54 (1999) 5809. | 632 |
| [5] | D. Rong, T. Mikami, M. Horio, Particle and bubble movements around tubes immersed in fluidized beds—a numerical study, <i>Chem. Eng. Sci.</i> 54 (1999) 5737. | 633 |
| [6] | K. Kuwagi, T. Mikami, M. Horio, Numerical simulation of metallic solid bridging particles in a fluidized bed at high temperature, <i>Powder Technol.</i> 109 (2000) 27. | 634 |
| [7] | K. Kuwagi, K. Takano, M. Horio, The effect of tangential lubrication by bridge liquid on the behavior of agglomerating fluidized beds, <i>Powder Technol.</i> 113 (2000) 287. | 635 |
| [8] | D. Rong, M. Horio, Behavior of particles and bubbles around immersed tubes in a fluidized bed at high temperature and pressure: a DEM simulation, <i>Int. J. Multiph. Flow</i> 27 (2001) 89. | 636 |
| [9] | B.J. Briscoe, C.R. McClune, The formation and geometry of entrapped liquid lenses at elastomer–glass interfaces, <i>J. Colloid Interface Sci.</i> 61 (1976) 485. | 637 |
| [10] | M.M.A. Safa, R. Gohar, Pressure distribution under a ball impacting a thin lubricant layer, <i>Trans. ASME J. Tribol.</i> 108 (1986) 372. | 638 |
| [11] | R.H. Davis, J. Serayssol, E.J. Hinch, The elastohydrodynamic collision of two spheres, <i>J. Fluid Mech.</i> 163 (1986) 479. | 639 |
| [12] | J. Serayssol, R.H. Davis, The influence of surface interactions on the elastohydrodynamic collision of two spheres, <i>J. Colloid Interface Sci.</i> 114 (1986) 54. | 640 |
| [13] | G. Barnocky, R.H. Davis, The effect of Maxwell slip on the aerodynamic collision and rebound of spherical particles, <i>J. Colloid Interface Sci.</i> 121 (1987) 226. | 641 |
| [14] | G. Lian, M.J. Adams, C. Thornton, Elastohydrodynamic collisions of solid spheres, <i>J. Fluid Mech.</i> 311 (1996) 141. | 642 |
| [15] | G. Lian, Y. Xu, W. Huang, M.J. Adams, On the squeeze flow of a power-law fluid between rigid spheres, <i>J. Non-Newton. Fluid Mech.</i> 100 (2001) 151. | 643 |
| [16] | J. Israelachvili, <i>Intermolecular and Surface Forces</i> , second edition, Academic Press, 1991. | 644 |
| [17] | L.M. Hocking, The effect of slip on the motion of a sphere close to a wall and of two adjacent spheres, <i>J. Eng. Math.</i> 7 (1973) 207. | 645 |
| [18] | H. Brenner, <i>Chem. Eng. Sci.</i> 16 (1961) 242. | 646 |
| [19] | D. Leighton, <i>Bull. Am. Phys. Soc.</i> 31 (1986) 1713. | 647 |
| | | 648 |
| | | 649 |
| | | 650 |
| | | 651 |
| | | 652 |
| | | 653 |
| | | 654 |
| | | 655 |
| | | 656 |
| | | 657 |
| | | 658 |
| | | 659 |
| | | 660 |
| | | 661 |
| | | 662 |
| | | 663 |
| | | 664 |
| | | 665 |
| | | 666 |
| | | 667 |
| | | 668 |
| | | 669 |
| | | 670 |
| | | 671 |
| | | 672 |